Carbohydrate Polymers 98 (2013) 495–504

Contents lists available at SciVerse ScienceDirect

Carbohydrate Polymers

journal homepage: www.elsevier.com/locate/carbpol

PAMAM conjugated chitosan through naphthalimide moiety for enhanced gene transfection efficiency

Kishor Sarkar, P.P. Kundu*

Department of Polymer Science & Technology, University of Calcutta, 92, A.P.C. Road, Kolkata 700009, West Bengal, India

ARTICLE INFO

Article history:
Received 21 April 2013
Received in revised form 4 June 2013
Accepted 7 June 2013
Available online xxx

Keywords:
Chitosan
PAMAM dendrimer
Cytotoxicity
In vitro
Transfection

ABSTRACT

Development of efficient and safe gene carrier is the main hurdle for successful gene therapy till date. Poor water solubility and low transfection efficiency of chitosan are the main drawbacks to be efficient gene carrier for successful gene therapy. In this work, PAMAM conjugated chitosan was prepared through naphthalimide moiety by simple substitution reaction. The synthesis of the chitosan conjugates was confirmed by FTIR, ^{1}H NMR and XRD analyses. The conjugates showed enhanced DNA binding capability compared to that of unmodified chitosan. Moreover, the conjugates showed minimal cytotoxicity compared to that of polyethyleneimine (PEI, 25 kDa) and also showed good blood compatibility with negligible haemolysis. The transfection efficiency of the conjugate was significantly increased compared to that of unmodified chitosan and it also surpassed the transfection efficiency by PEI. Therefore, PAMAM conjugated chitosan can be used safely as alternate efficient gene delivery vector in gene therapy.

1. Introduction

Gene therapy has become a promising alternative clinical approach to treat genetic diseases like Alzheimer (Nilsson et al., 2010), Parkinson's disease (Denyer & Douglas, 2012), cardiovascular problems (Dishart, Work, Denby, & Baker, 2003) and even cancer (Cross & Burmester, 2006). However, efficient and safe gene carrier is the main hurdle for successful gene therapy (Lechardeur & Lukacs, 2002; Niidome & Huang, 2002; Zhou, Liu, & Liang, 2004). Although viral vectors have been used as most powerful carriers for gene delivery to treat various intractable diseases (Daya & Berns, 2008; Jia & Zhou, 2005; Stone, David, Bolognani, Lowenstein, & Castro, 2000; Waehler, Russell, & Curiel, 2007; Walther & Stein, 2000) but their immunogenic and carcinogenic characteristics limit their practical use in human (Sun, Chatterjee, & Wong, 2002; Thomas, Ehrhardt, & Kay, 2003). In contrast, nonviral vectors such as cationic lipids (Miller, 1998; Pedroso de Lima, Neves, Filipe, Düzgüneş, & Simões, 2003; Simões et al., 2005) and cationic polymers (He, Tabata, & Gao, 2010; Merdan, Kopecek, & Kissel, 2002; Morille, Passirani, Vonarbourg, Clavreul, & Benoit, 2008; Samal et al., 2012) have gained tremendous attention as alternate vector for gene carrier due to low immunogenicity, high chemical structure versatility and low production cost; although low transfection ability of these nonviral vectors is still insufficient to elicit systemic therapeutic effects (Li & Huang, 2006; Pérez-Martínez, Guerra, Posadas, & Ceña, 2011; Romano, 2007). Positively charged cationic polymer can condense negatively charged DNA into nanosized particle due to electrostatic interaction and effectively prevent DNA from nuclease degradation (Jewell & Lynn, 2008). Polyethyleneimine (PEI) is the most widely used nonviral vector among the cationic polymers due to its high transfection efficiency (Lungwitz, Breunig, Blunk, & Göpferich, 2005; Wightman et al., 2001), but severe toxicity limits its clinical application (Hunter & Moghimi, 2010; Moghimi et al., 2005). On the other hand, chitosan has become a promising contender as alternate nonviral vector because of its natural source, biodegradability, biocompatibility and very low toxicity (Kundu & Sarkar, 2011; Muzzarelli, 2010a, 2010b). However, low specificity and low transfection efficiency of chitosan are the main drawbacks for clinical trials (Huang, Fong, Khor, & Lim, 2005). Due to the presence of various functional groups such as primary amine groups, hydroxyl groups on the backbone of chitosan, it can be chemically modified to get the desired property. A variety of chitosan derivatives have been synthesized such as PEGylated chitosan (Jiang et al., 2006), quaternized chitosan (Thanou, Florea, Geldof, Junginger, & Borchard, 2002), oligoamine-conjugated-chitosan (Lu, Sun, Li, Zhang, & Zhuo, 2009), trimethylated chitosan (Kean, Roth, & Thanou, 2005), etc. to improve its solubility or gene transfection efficiency.

Dendrimers are relatively new class of synthetic, highly branched, nanospherical well-defined architectures with precise molecular weight, multivalent functionalization sites and low dispersity index macromolecules (Svenson & Tomalia, 2005; Tomalia

* Corresponding author. Tel.: +91 2350 1397; fax: +91 2350 1397.
E-mail address: ppk923@yahoo.com (P.P. Kundu).

0144-8617/$ – see front matter © 2013 Elsevier Ltd. All rights reserved.
http://dx.doi.org/10.1016/j.carbpol.2013.06.006

& Frechet, 2005). Poly(amidoamine) (PAMAM) dendrimer has been attracted interest as nucleic acid delivery vectors (Dufes, Uchegbu, & Schatzlein, 2005) due to its uniformity in size with high density of primary amine groups at the surface. However, severe cytotoxicity of PAMAM dendrimers limits their widespread use in drug and gene delivery applications (Sadekar & Ghandehari, 2012); although higher generation PAMAM dendrimers show higher cytotoxicity and haemolysis compared to that of lower generation dendrimers (Mukherjee, Davoren, & Byrne, 2010). To keep this thought in mind, low generation PAMAM dendrimer (generation 2, G2) conjugated chitosan was prepared in this work. In our previous study (Sarkar & Kundu, 2012), chitosan-*graft*-PAMAM copolymer was prepared through N-maleation of chitosan and the copolymer with G2 PAMAM dendrimer showed comparatively lower cytotoxicity than that of G3 PAMAM dendrimer. Here, we prepared PAMAM conjugated chitosan through naphthalimide moiety by simple substitution reaction. Then, the synthesized conjugates were assessed for DNA complexation, in vitro cytotoxicity, in vitro transfection in HeLa cell line and blood compatibility was also investigated.

2. Experimental

2.1. Materials

Low molecular weight chitosan (55 kDa, DDA 82%) was prepared from high molecular weight chitosan (365 kDa, Himedia, India) by oxidative degradation with sodium nitrite (Merck, India) at room temperature according to our previous method (Sarkar & Kundu, 2012). The molecular weight and degree of deacetylation (DDA) of chitosan were determined by gel permeation chromatography (Waters 2414 RI detector, PC2 separation module, using empower 2 software against PEG standard (sigma) calibration curve) and potentiometric titration method (Sarkar, Srivastava, Chatterji, & Kundu, 2011), respectively. 4-Bromo-1,8-naphthalic anhydride was purchased from Sigma–Aldrich. Specially dried DMSO was obtained from Merck, India. PAMAM dendrimer of generation 2.0 was prepared by Michael addition reaction between ethylene diamine (EDA) (Merck, India) as core molecule and methyl acrylate (MA) (Merck, India) followed by amidation reaction between the ester terminated half generation PAMAM dendrimer and EDA according to our previous report (Sarkar & Kundu, 2012). DNase I (1 unit/μl) was purchased from Fermentas, Thermo Scientific, India. Dulbecco's modified Eagle's medium (DMEM), penicillin–streptomycin, trypsin, fetal bovine serum (FBS) were obtained from Himedia Laboratories Pvt. Ltd., India. 3-(4,5-Dimethylthiazol-2-yl)-2,5-diphenyltetrazolium bromide (MTT) and agarose were purchased from Sisco Research Laboratories Pvt. Ltd., India. pEGFP-N1 control vector (4.7 kb containing SV-40 promoter) was kindly donated by Dr. Gopal Chakroborty, Department of Biotechnology, University of Calcutta. The plasmids were propagated in *Escherichia coli* (*E. coli*) and the plasmid DNA (pDNA) was isolated with QIAGEN Midiprep pDNA isolation Kit (USA) according to the manufacturer's instructions. Its purity was confirmed by spectrophotometry (A_{260}/A_{280}) and its concentration was determined from its absorbance at 260 nm. All other reagents were analytical grade and were used directly without further modification.

2.2. Preparation of N-(4-bromonaphthalimide)-chitosan 3

N-(4-bromonaphthalimide)-chitosan was prepared according to our previous method (Sarkar, Debnath, & Kundu, 2013) with slight modification. Briefly, 2 g chitosan was suspended into 100 mL DMSO and then 0.35 g of 4-bromo-1,8-naphthalic anhydride **2** was added to the above suspension. The reaction mixture was refluxed at 80 °C under nitrogen atmosphere for 3 h. Then, the reaction mixture was filtered in hot condition and washed with hot DMSO to remove unreacted 4-bromonaphthalic anhydride. Finally, the product was washed successively with water, methanol and acetone and then vacuum dried at 50 °C for 24 h to get brown colored compound **3** (yield 86.6%).

2.3. Preparation of N-naphthalimide chitosan-PAMAM conjugates *4*

N-naphthalimide chitosan-*conjugate*-PAMAM was prepared by heterogeneous method as per our previous study (Sarkar et al., 2013). 100 mg of compound **3** was dispersed in 50 mL aqueous solution of PAMAM dendrimer with different concentrations (10%, 20% and 40%) to prepare different substituted chitosan conjugates. The reaction mixture was then refluxed at 80 °C under nitrogen atmosphere for 3 h. The product was filtered and washed with water, methanol and acetone. Finally, the product was dried under vacuum at 50 °C for 24 h to get yellow colored compound **4** (yield 84.2%).

2.4. Characterization of the polymers

Fourier transform infrared (FTIR) analysis was carried out with ATR FTIR spectroscopy (model-Alpha, Bruker, Germany). The sample was uniformly mixed with potassium bromide at 1:10 weight ratio and KBr pellets were prepared using 10 ton hydraulic pressure for 10 min at room temperature. Then, FTIR spectra of the pellets were carried out within the frequency range of 4000–500 cm^{-1} for 42 consecutive scans. The ^1H nuclear magnetic resonance (1H NMR) spectra were determined on a Bruker AV 3000 Supercon NMR system (Germany) at 300 MHz using D_2O/DCl and D_2O as solvent. Chemical shifts (δ) were reported in ppm using tetramethylsilane (TMS) as an internal reference. The degree of substitution (DS) value was calculated according to the following equation:

$$\mathrm{DS} = \frac{\text{integrated area at } 2.4 - 2.8 \text{ ppm}}{16 \times \text{integrated area at } 3.1 \text{ ppm}}$$

X-ray diffraction spectrometry of the polymers in the powder form was performed by a wide angle X-ray scattering diffractometer (Panalytical X-Ray Diffractometer, model-X'pert Powder) with Cu K_α radiation ($\lambda = 1.544$) in the range 5–50° (2θ) at 40 kV and 30 mA. Fluorescent spectra of chitosan and compound **4c** were measured by JASCO FP-8000 spectrofluorometer.

2.5. Preparation of polymer/DNA complexes

Polymer/DNA complexes were prepared by complex coacervation method. Both chitosan (CTS) and compound **4c** were dissolved in acetic acid/sodium acetate buffer at pH 5.5 with a concentration of 2 mg/mL and the solutions were filtered by Millipore 0.45 μm filter paper. pDNA was dissolved separately (100 μg/mL) in 25 mM of sodium sulphate solution. The polymer solutions were then diluted with buffer to get the desired concentration for complex formation. Both the polymer and DNA solutions were preheated separately at 50–55 °C for 10 min. Then, complexes at different N/P ratios (nitrogen to phosphate ratio) were prepared by immediate mixing of equal volume of polymer and pDNA solution and subsequently vortexing for 15–30 s with cyclomixer (REMI, India). After that, the resulting mixtures were incubated at room temperature for 30 min for complete formation of complexes. The binding ability of polymer with pDNA was determined by agarose gel (0.8%) electrophoresis (100 V for 45 min). The picture of the gel was subsequently captured by BIOTOP gel doc system (Shanghai, China).

2.6. Determination of particle size and zeta potential

The particle size and distribution as well as surface charge of the complexes at different N/P ratios were determined by dynamic light scattering (DLS). The solutions were filtered through a 0.45 μm filter (Millipore) prior to the experiment to avoid the influence of dust on the reliability of results. The DLS measurement was carried with Zetasizer Nano ZS (Malvern Instrument, UK) at 37 °C. The zeta potentials of the complexes were measured using the same instrument.

2.7. Atomic force microscopy measurement

The size and morphology of CTS-PAMAM conjugate/pDNA nanoparticles were also characterized by AFM (Nanoscope IV Bioscopet, Digital Instruments, Veeco). 1–2 μL of samples containing complexes in acetate buffer with a final DNA concentration of 100 μg/mL was deposited onto the center of a freshly split untreated mica disk. The mica surface was then dried at room temperature before imaging. The imaging was conducted with silicon nitride tip in tapping mode and a scan speed of 1 Hz at ambient condition.

2.8. Buffering capacity

The buffering capacity of chitosan, compound **4**, PAMAM (G2) dendrimer and PEI 25 kDa were measured by acid–base titration assay between pH 10 and 2.0. The samples were dissolved in 30 mL of 150 mM NaCl solution (pH 7.4). The solution was first titrated by 0.1 M NaOH to a pH of 10.30; then 0.1 M HCl was gradually added to the solution and consequently the pH was measured using a pH meter (Make-CD, India, Model: APX175 E/C).

2.9. Blood compatibility

Human blood was collected from healthy male adults (25–31 years old). A total of 200 μl of the whole blood was added to different amounts of polymer solutions and the volume was adjusted to 1 mL with sterile PBS solution (pH = 7.4). The blood compatibility test in PBS solution and in Triton X-100 solution (1%, v/v) were used as negative and positive controls, respectively. After incubation at 37 °C for 90 min, the solutions were centrifuged at 2000 rpm for 10 min. A total 200 μl of the supernatant was collected and seeded in each well of 96 wells plate. The absorbance was recorded on ELISA micro plate reader (Multiskan EX, Labsystems, Helsinki, Finland) at a wavelength of 543 nm. The percentage hemolysis (PH%) was calculated using the following equation:

$$\mathrm{PH\%} = \frac{A_s - A_p}{A_n - A_p} \times 100$$

where A_s, A_n and A_p are the absorbance of sample, negative and positive controls, respectively.

2.10. DNase I digestion assay

pDNA protection capability of the polymer against enzyme was carried out by DNase I (used as model enzyme) digestion assay. Naked pDNA and polymer/pDNA complexes against DNase I (1 unit/l μg of DNA) were assayed in 2 mL of 10 mM phosphate buffered saline (PBS) containing 5 mM $MgCl_2$ at 37 °C. At first, polymer/pDNA complexes and naked pDNA were incubated with 1 μL of DNase I for 10 min at 37 °C and then, DNase I was inactivated by adding 0.5 M EDTA. The degradation of DNA was investigated by 0.8% agarose gel electrophoresis.

2.11. In vitro cytotoxicity assay

Cytotoxicity of chitosan and CTS-PAMAM conjugate was determined on HeLa cells by MTT assay. HeLa cells were seeded into 96-well culture plates at a density of 1×10^4 cells per well. After 24 h incubation, the cells were treated with CTS, CTS conjugates, PAMAM dendrimer (G2) and polyethyleneimine (PEI) as control polymer with final concentrations of 5, 10, 25, 50, 75, 100, 150, 200 and 300 μg/mL and incubated for another 24 h. Untreated cells in growth media were used as the blank control. Then, 20 μL of 3-(4,5-dimethylthiazol-2-yl)-2,5-diphenyltetrazolium bromide (MTT) solution (5 mg/mL) in PBS buffer was added to each well. After further incubation for 4 h, the media was removed and replaced with 100 μL DMSO to dissolve the MTT formazan crystals. The absorbance was recorded at 570 nm by an ELISA microplate reader (Multiskan EX, Labsystems, Helsinki, Finland). The cell viability (%) was calculated according to the following equation:

$$\text{cell viability}\,(\%) = \left\{100 - \frac{A_s - A_b}{A_c - A_b}\right\} \times 100$$

where A_s, A_b and A_c are the absorbance value of sample, blank and control, respectively. All data are presented as the mean of six measurements (±SD).

2.12. In vitro transfection studies

HeLa cells were seeded in 6-well plates at the density of 1×10^3 cells/well in 1 mL of complete media (DMEM high glucose supplemented with 10% FBS) and incubated for 24 h at 37 °C in a humidified atmosphere containing 5% CO_2 until the cells were approximately 80% confluent. The polymer/DNA complexes were prepared at different N/P ratios according to the above procedure (containing 2 μg DNA in each N/P ratio) prior to the transfection. Two hours before the transfection, the complete growth media was replaced with fresh media without FBS and antibiotics. The polymer/DNA complexes containing 2 μg DNA at different N/P ratios were added into each well and were incubated at 37 °C in a CO_2 incubator for another 4 h. Then, the transfection media was replaced with complete growth media and incubated for 24 h. All transfection studies were carried out in triplicate. Naked DNA and PEI/DNA (N/P = 10) were used as negative control and positive control, respectively. The cells were analyzed after 24 h post incubation for enhanced green fluorescence protein (pEGFP-N1) expression with a fluorescence microscope (OLYMPUS IX70, Japan).

For flow cytometric analysis, pEGFP-N1 transfected cells were harvested through trypsinization. Then, the cells were resuspended into 1X PBS buffer at pH 7.4 and the suspensions were then transferred to 5 mL flow cytometry tubes. EGFP expression in the transfected cells was quantified using a Becton–Dickinson FACS scan instrument and the data were analyzed using Cell Quest program from Becton–Dickinson. For each sample, 10,000 events were counted and the green fluorescence of EGFP was detected through 525/530 nm (FL1) band pass filter.

2.13. Statistical analysis

All experiments were repeated in triplicate unless otherwise noted. Statistical analysis was performed using Student's *t*-test and differences were judged to be significant at $p < 0.05$.

3. Result and discussion

3.1. Preparation and characterization of chitosan conjugates

In order to synthesize of chitosan-PAMAM conjugate by conjugating of PAMAM (G2) dendrimer with chitosan,

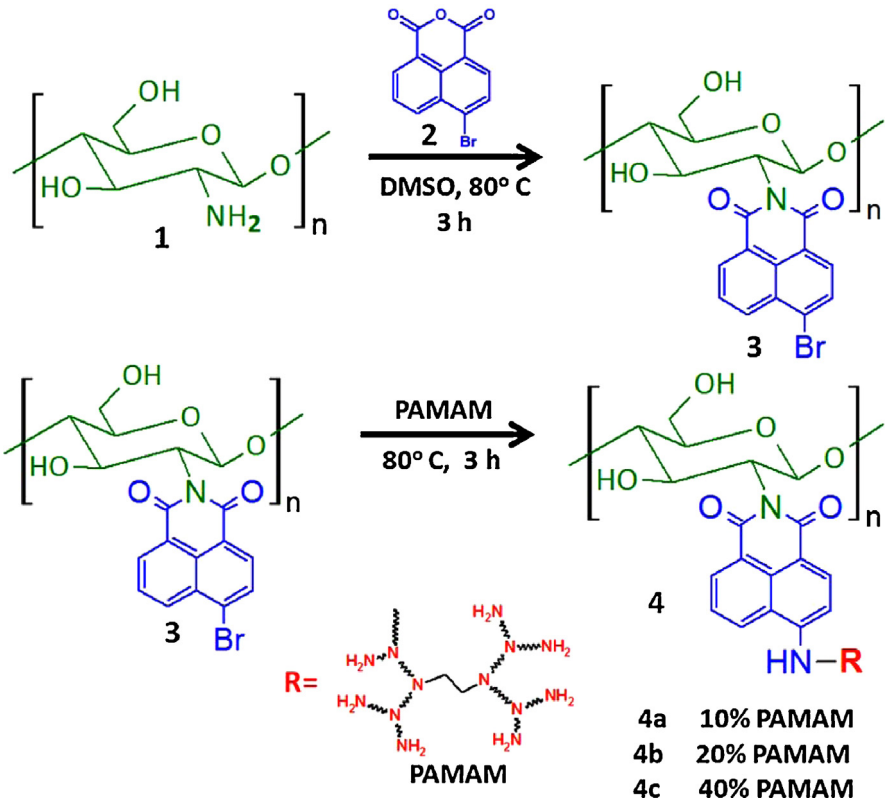

Fig. 1. Synthetic route for the synthesis of chitosan-PAMAM conjugate.

4-bromo-1,8-naphthalic anhydride was firstly introduced on to chitosan through primary amine groups to prepare N-(4-bromonaphthalimide)-chitosan (compound **3**) followed by addition of PAMAM dendrimer through substitution of bromine group of bromonaphthalimide chitosan by the primary amine groups of PAMAM dendrimer to prepare compound **4**. The synthetic route of PAMAM conjugated chitosan copolymer preparation is shown in Fig. 1. FTIR spectra of CTS, 4-bromonaphthalic anhydride, compound **3** and compound **4c** are shown in Fig. 2. As shown in Fig. 2a, the main characteristic peaks of CTS are: 3422.55 cm^{-1} (wide peak of O—H stretching overlapped with N—H stretching), 1652.98 cm^{-1} (NH—CO (I) stretch), 1597.16 cm^{-1} (N—H bend), 1155.46 cm^{-1} (bridge —O— stretch) and 1095.16 cm^{-1} (bridge C—O—C stretching and C—O stretching). Fig. 2b shows the symmetric and antisymmetric C=O stretches of compound **2** at 1777.16 and 1731.86 cm^{-1}, respectively. After reaction between CTS and 4-bromonaphthalic anhydride, the peaks for C=O stretch and N—H bend of 4-bromonaphthalic anhydride are changed to 1702.00 cm^{-1} and 1662.67 cm^{-1}, respectively in compound **3** (Fig. 2c) due to the conversion of some primary amine groups of chitosan to imide groups. The characteristic peaks obtained for compound **4c** are: 3444.40 cm^{-1} (wide peak of O—H stretching overlapped with N—H stretching), 2923.27 cm^{-1} (C—H stretching), 1661.46 cm^{-1} (amide II band, N—H bending and C—O stretching of acetyl groups), 1424.44 cm^{-1} (O—H bending, C—N stretching, asymmetric C—H bending of CH_2 group), and 1092.75 cm^{-1} (bridge C—O—C stretching and C—O stretching). The peak at 3511.35 cm^{-1} for compound **3** has shifted to lower wave number (3444.40 cm^{-1}) and becomes more intense after PAMAM conjugating due to increasing the number of primary amine groups in compound **4c**. The other change in spectral peak was noted within the spectral range between 1156.02 cm^{-1} and 1031.20 cm^{-1} after PAMAM conjugating with compound **3** through naphthalimide moiety.

The ^1H NMR spectra of chitosan and compound **4c** are shown in Fig. 2e and f. In Fig. 2e, typical peaks at 3.4–4.0 ppm are assigned to glucosamine unit (H3, H4, H5, H6) of chitosan, the peak at 3.1 ppm is responsible for H2 and the peak at 2.1 ppm is assigned to the methyl protons of N-acetyl group. After the reaction between compound **3** and PAMAM (40%) dendrimer, new broad peaks with multiplicity are appeared at 7.6–9.0 ppm and 2.4–3.5 ppm in the NMR spectrum of compound **4c** (Fig. 2f) attributed to aromatic protons of naphthalimide moiety and the methylene protons of PAMAM, respectively and the degree of substitution was 0.42.

It was also found that the solubility of compound **3** was slightly decreased after the reaction between chitosan and compound **2** due to the incorporation of hydrophobic aromatic moiety into the chitosan molecule and consequently decreasing the number of primary amine groups. But, the solubility of compound **3** was markedly improved after conjugating of PAMAM dendrimer with compound **3** (Table 1). As shown in Table 1, the solubility of compound **4** was increased with increasing the degree of substitution

Table 1
Degree of substitution (DS) and solubility of chitosan and chitosan derivatives.

Compound	DS[a]	Solubility	
		H_2O	0.1 M HCl
CTS	–	I	S
Compound **3**	0.05	I	P
Compound **4a**	0.12[b]	P	S
Compound **4b**	0.29[b]	P	S
Compound **4c**	0.42[b]	S	S

I, insoluble; S, soluble; P, partly soluble.
[a] Determined by NMR.
[b] DS value of compound **4** was calculated based on compound **3**.

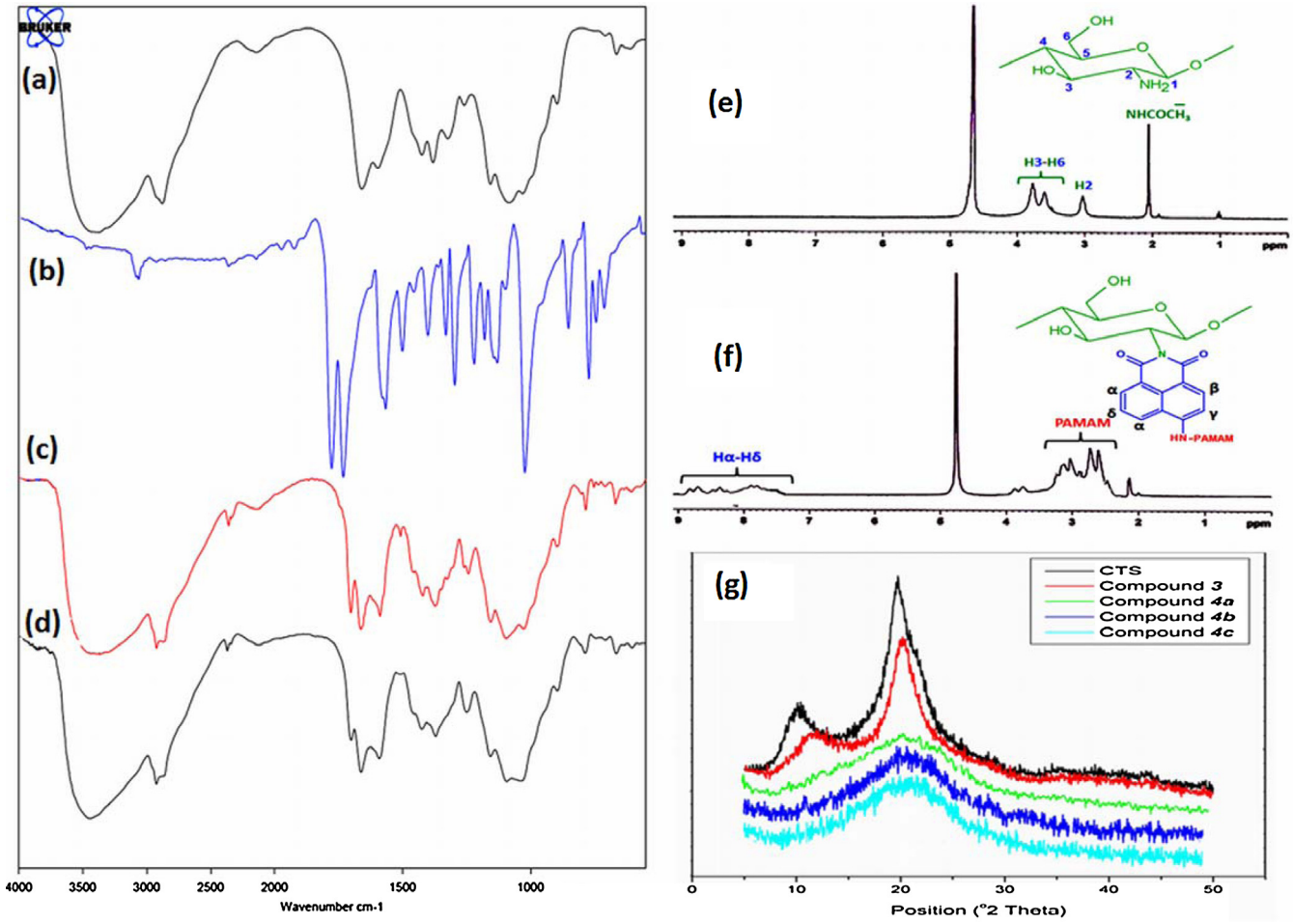

Fig. 2. FTIR spectra of chitosan (a), compound **2** (b), compound **3** (c) and compound **4c** (d); ^{1}H NMR spectra of chitosan (e), compound **4c** (f); and X-ray diffraction patterns of chitosan and its conjugates (g).

(DS) value because the number of primary amine groups was significantly increased after conjugating of PAMAM with compound **3**. Although, we obtained less soluble product when we used lower amount of PAMAM (10%) but we got soluble product when excess of PAMAM (40%) was used. This phenomenon can be explained by the fact that when, lower amount of PAMAM dendrimer was used, the free primary amine groups of chitosan in compound **3** took part in competitive substitution reaction with the primary amine groups of PAMAM dendrimer and could substitute the bromine group of compound **3** to form cross-linked product. But, when large excess amount (40%) of PAMAM dendrimer was used, due to smaller molecular size of PAMAM molecule compared to that of compound **3**, PAMAM molecule preferentially reacted with compound **3** to form the soluble product compound **4c** by the substitution reaction. Similar results were obtained in our previous study (Sarkar & Kundu, 2012).

The X-ray diffraction of chitosan and its derivative is shown in Fig. 2g. Chitosan showed two different peaks at $2\theta = 10^\circ$ and $2\theta = 20^\circ$. The peak at 10° was assigned to crystal form I and the strong peak at 20° was assigned to crystal form II of chitosan (Sarkar, Debnath, & Kundu, 2012). But, for chitosan derivatives, the intensity of the peaks at 10° and 20° was significantly decreased. The reason may be attributed to the destruction of the intermolecular hydrogen bonds between the amine groups and hydroxyl groups of chitosan due to the conjugation. These results indicate that the conjugation caused destruction of the ordered crystal structure of the chitosan.

The formation of compound **3** and compound **4** was further confirmed by sperctrofluorometer. The fluorescence spectrum of compound **3** and compound **4c** is shown in Fig. 3A. From Fig. 3A, it is found that both compounds **3** and **4c** showed the excitation (inset) at the same wave length of 350 nm but the compound **4c** exhibited the red shift of 5 nm (λ_{max} = 410 nm for compound **3**) compared to that of compound **4c** (λ_{max} = 405 nm).

3.2. Preparation of polymer/DNA complex

The ability of the polymers to bind DNA due to electrostatic interaction between the positively charged polymer and negatively charged DNA was evaluated using agarose gel retardation assay. Fig. 3B shows the agarose gel electrophoresis assay of chitosan/pDNA complexes and compound **4**/pDNA complexes. The electrophoretic mobility of plasmid DNA was completely retarded by chitosan at comparatively higher N/P ratio 3.0 (Fig. 3A, a) but the pDNA retardation capability of chitosan was markedly improved after conjugating of PAMAM dendrimer with chitosan. Compound **4c** showed better DNA binding capability than compounds **4a** and **4b** due to higher DS value and compound **4c** complexed all pDNA at very low N/P ratio (N/P ratio = 1.0) where no free DNA was found in the lane (Fig. 3B, d). This may be explained by the fact that compound **4c** has gained higher positive charge density than chitosan and compounds **4a** and **4b** due to higher substitution degree that increases the number of primary amine groups at the outer surface of the compound **4c** and consequently the complexation

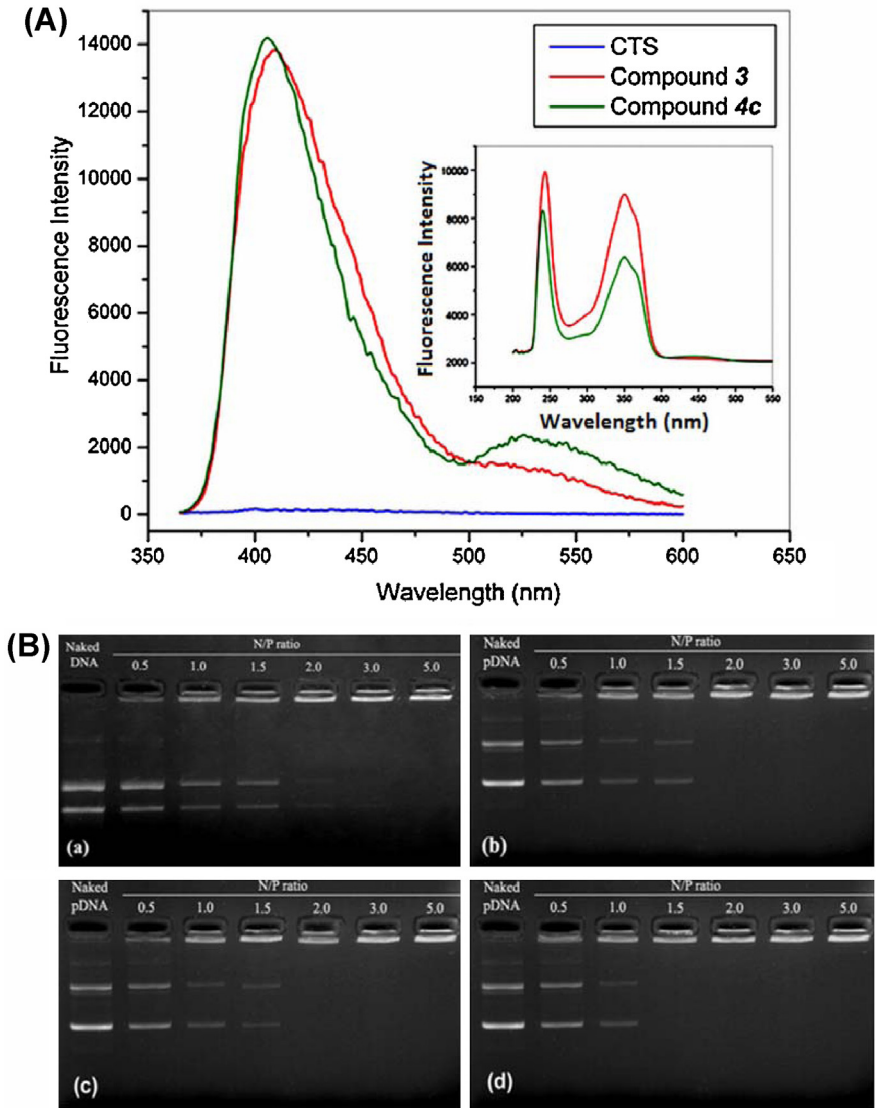

Fig. 3. (A) Fluorescence emission spectra of chitosan, compound **3** and compound **4c** and excitation spectra (inset) and (B) agarose gel electrophoresis of chitosan/pDNA complex (a), compound **4a**/pDNA complex (b), compound **4b**/pDNA complex (c) and compound **4c**/pDNA complex (d).

capability of the conjugate increased with the negatively charged pDNA.

3.3. *Particle size and zeta potential*

Particle sizes and zeta potentials of the cationic polymer/pDNA complexes are important parameters for efficient gene delivery. Fig. 4A shows the particle sizes (a) and zeta potentials (b) of chitosan/pDNA and compound **4c**/pDNA complexes in PBS buffer (pH 7.4) at different N/P ratios. From Fig. 4A, a, it is found that the particle sizes of all complexes decreased with increasing the N/P ratio from 0.5 to 3.0. After reaching the N/P ratio of 3.0, the particle sizes increased slightly with further augmentation of N/P ratios for both chitosan and compound **4c** and this phenomenon might be attributed to the repulsion of excessive positive charges provided by polymers. Although, CTS-PAMAM conjugate formed the smallest particles comparatively at lower N/P ratio (N/P ratio = 1.5) within the size range of 155–190 nm whereas unmodified chitosan formed smaller particles at higher N/P ratio (N/P ratio = 3.0) and the particle sizes were in the range of 200–220 nm.

Zeta potential, an indicator of surface charges on the polymer/pDNA complexes, is another important factor affecting cellular uptake of the complexes. A positively charged surface allows electrostatic interaction with negatively charged cell surfaces and facilitates cellular uptake. Zeta potentials of the chitosan/pDNA and compound **4c**/pDNA complexes were measured in PBS buffer (pH 7.4) at various N/P ratios. As shown in Fig. 4A, b, the zeta potentials for chitosan/pDNA and compound **4c**/pDNA complexes at N/P ratios below 2 and 1.5, respectively were negative which implies incomplete complexation. With increasing N/P ratio, zeta potentials of both complexes rapidly increased and reached almost plateau at N/P ratios between 3 and 7. The compound **4c**/pDNA complexes showed the highest zeta potential value of 30 mV, while the unmodified chitosan/pDNA showed the zeta potential of 19 mV at N/P ratio of 7.

The particle size and morphology of CTS-PAMAM conjugate/pDNA complexes were further characterized by AFM study (Fig. 4B). As shown in Fig. 4B, compound **4c** formed spherical shaped nanoparticles with pDNA at both N/P ratios (N/P ratio 1.5 and 3.0) but it formed comparatively smaller particle at N/P ratio 1.5 and

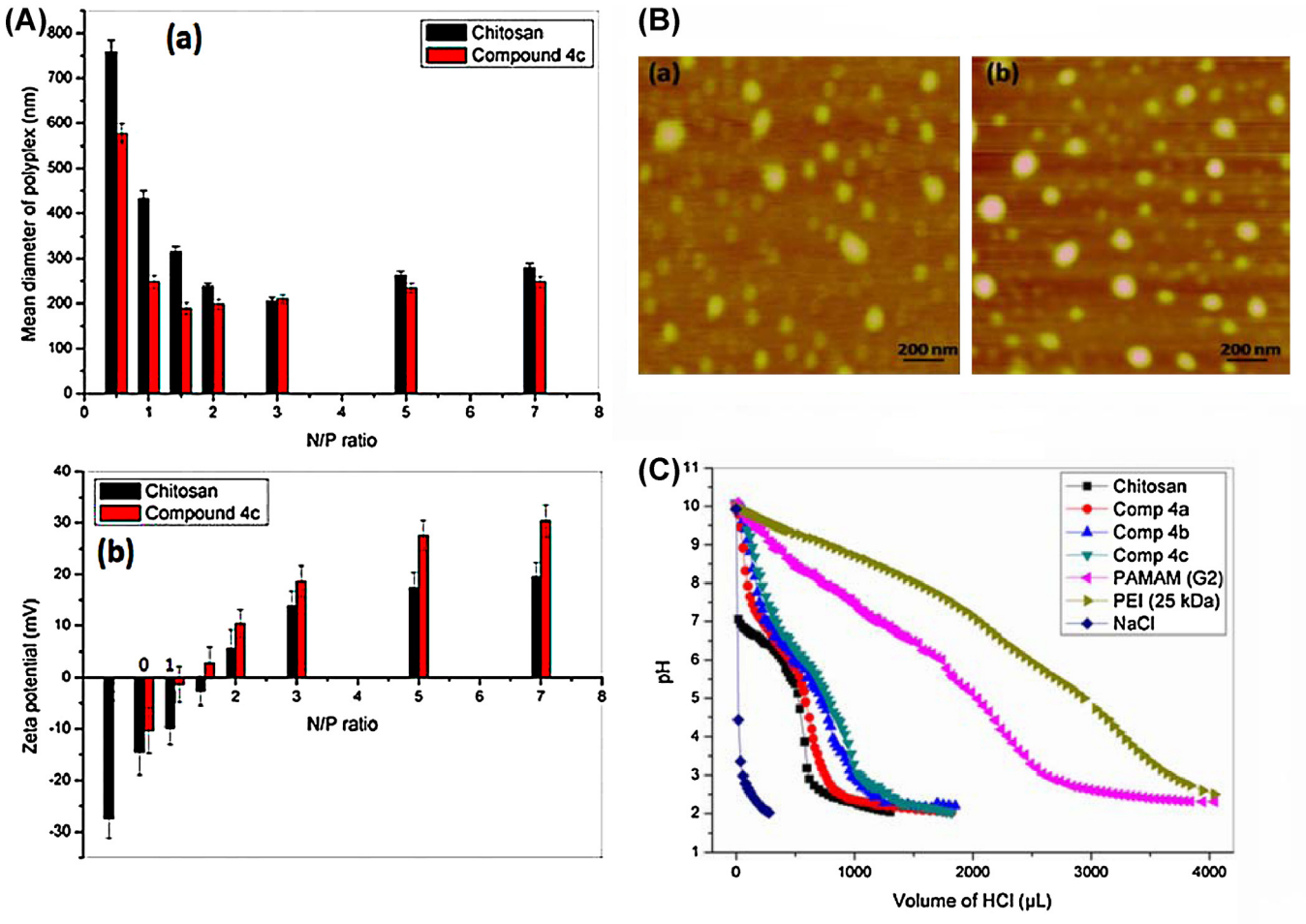

Fig. 4. (A) DLS particle size of CTS/pDNA and CTS-PAMAM conjugate/pDNA complexes (a) and zeta potential of CTS/pDNA and CTS-PAMAM conjugate/pDNA complexes (b) at different N/P ratios. Data are shown as mean ± SD ($n = 3$); (B) AFM micrographs of CTS-PAMAM conjugate/DNA complexes at N/P ratios of **2** (a) and **3** (b); and (C) buffer capacity of chitosan, compound **4a**, **4b**, and **4c**, PAMAM (G2) and PEI (25 kDa) in 150 mM NaCl solutions.

the particle size was in the range of 80–120 nm which are in very good agreement with the particle sizes obtained from DLS study.

3.4. Buffering capacity

The buffering capacity of CTS-PAMAM conjugate was determined by acid–base titration of the polymer. The buffering capacity versus pH profile of chitosan, compound **4**, PAMAM (G2) and PEI (25 kDa) was compared as given in Fig. 4C. The titration curve shows that the buffering capacity of chitosan was markedly increased after conjugating of PAMAM dendrimer onto chitosan backbone. Unmodified chitosan showed very poor buffering capacity and the acid–base titration of unmodified chitosan was started from pH 7.0 because chitosan is insoluble at pH 7.4. But, PEI and PAMAM dendrimer showed higher buffering capacity due to the presence of large number of primary, secondary and tertiary amine groups. So, the buffering capacity of chitosan was increased after conjugating PAMAM dendrimer onto chitosan backbone due to increase in the primary amine groups in the conjugate. Compound **4c** showed maximum buffering capacity among the other conjugates because of its high DS value.

3.5. Blood compatibility

In vitro hemolysis assay is considered to be a simple and reliable measure for estimating blood compatibility of materials. The in vivo applicability of the biomaterials can be predicted by investigating the degree of hemolysis in vitro. In this study, we compared the percentage hemolysis of CTS-PAMAM conjugates with that of chitosan, PAMAM (G2) and PEI (25 kDa) at different concentrations in the range of 0.01–10 mg/mL. Phosphate buffered saline (PBS) at pH 7.4 and Triton X-100 (1%, v/v) solutions were used as a negative and positive control, respectively. Fig. 5b demonstrates the percent hemolysis results. From Fig. 5b, it is found that a slight hemolysis was produced in all conjugates after 90 min incubation, although the amount of hemolysis was negligible compared to that of PEI (25 kDa) and PAMAM (G2). Unmodified chitosan showed a negligible hemolysis (less than 2%). Whereas, PEI was found to be the most membrane damaging polymer reaching complete hemolysis of the hemoglobin at a concentration ≥1 mg/mL and PAMAM (G2) dendrimer caused 21% hemolysis at a concentration of 10 mg/mL. Compound **4c** showed maximum hemolysis among the conjugates because of its higher DS value, although the amount of hemolysis was significantly low compared to that of PEI and PAMAM dendrimer.

3.6. DNase I digestion assay

For successful gene therapy application, DNA stability against degradation by nucleases is an important issue. Because, deoxyribonuclease I (DNase I) or DNase I like enzymes exist in the extracellular space and cellular cytoplasm and they play an important role in DNA degradation and disruption during gene delivery.

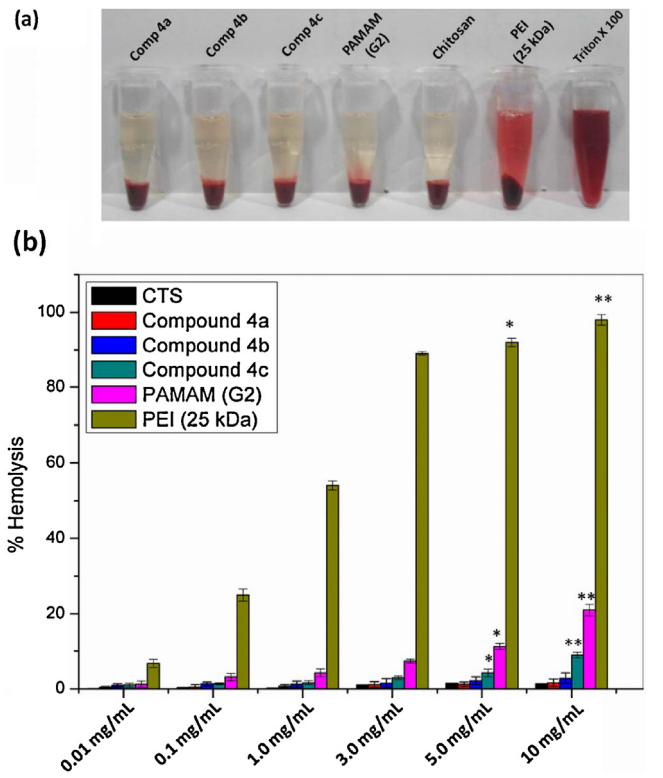

Fig. 5. Visual observation of hemolysis caused by CTS-PAMAM conjugates, PAMAM (G2), CTS, PEI (25 kDa) in phosphate buffer at pH 7.4 and Triton X 100 (a) and bar graph of % hemolysis by different polymers at concentration range 0.01–10 mg/mL (b). PBS buffer at pH 7.4 was used as negative control and Triton X 100 (1%, v/v) was used as positive control. Data are shown as mean ± SD ($n = 3$).

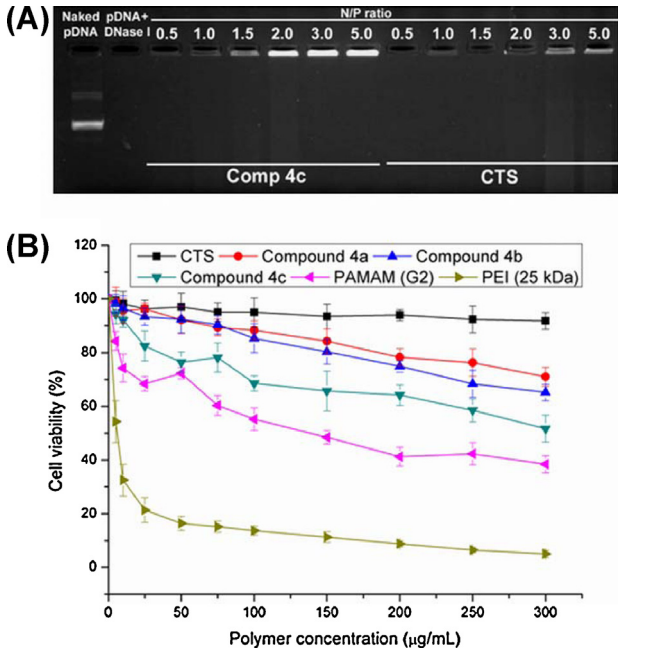

Fig. 6. DNase I assay of compound **4c**/pDNA and CTS/pDNA complexes at different N/P ratios (A) and cell viabilities of CTS, compounds **4a**, **4b** and **4c**, PAMAM (G2) dendrimer and PEI at different concentration in HeLa cell line (B). Data are shown as mean ± SD ($n = 6$).

Therefore, it is necessary to investigate the ability of synthetic vector to protect the genetic material from degradation during its transport to the target cells. DNase I protection assay is a general procedure to evaluate the nuclease protection of pDNA. Fig. 6A shows the protection capability of chitosan and compound **4c** against pDNA degradation by DNase I. As shown in Fig. 6A, naked plasmid DNA was completely digested by DNase I at 1 unit/μg (lane 2) indicating the reactivity of DNase I against DNA degradation. In contrast, compound **4c** efficiently protected pDNA from nuclease digestion at or above N/P ratio 1.5, whereas CTS protected the pDNA at comparatively higher N/P ratio 3.0. Our studies showed that compound **4c** could protect DNA efficiently against degradation by DNase I, which is one of the crucial factors for efficient gene delivery in vitro as well as in vivo.

3.7. In vitro cytotoxicity

Minimum cytotoxicity of polymeric vectors is an important parameter for in vivo application. We investigated the cytotoxicity of chitosan, conjugates, PAMAM (G2) dendrimer and PEI (25 kDa) at various concentrations (5, 10, 25, 50, 75, 100, 150, 200, 250 and 300 μg/mL) by MTT assay on HeLa cells (Fig. 6B). Cells without treatment of polymer were used as a control with cell viability assumed to be 100%. As shown in Fig. 6B, it was observed that the cell viability of HeLa was above 90% in the presence of chitosan even at high concentration (300 μg/mL). On the other hand, CTS-PAMAM (G2) conjugates showed little toxicity toward the cell line at low concentrations (up to 75 μg/mL), where above 80% cells were viable. But, the cell viability decreased with further increasing the polymer concentration although, the cells were above 50% viable at higher concentration (300 μg/mL). The cytotoxicity of polycations is probably due to strong electrostatic interaction with the plasma membrane, which results in destabilization by aggregation on the cell surfaces and ultimately impairs the cell membrane functions. On the contrary, branched PEI (25 kDa) showed significant toxicity to the cells and the cell viability reached to 20% at very low polymer concentration of 25 μg/mL whereas, the conjugates showed above 80% cell viability at the same concentration. It is also found from Fig. 6B that PAMAM (G2) dendrimer showed around 50% and 40% cell viability at concentrations of 100 μg/mL and 300 μg/mL, respectively which was higher than PEI but lower than the conjugates. But, the toxicity of PAMAM dendrimer decreased after conjugating with chitosan backbone. Our previous report showed the similar result where branched PEI was conjugated with chitosan through naphthalimide moiety (Sarkar et al., 2013). Therefore, PAMAM conjugated chitosan may be considered as alternate biomaterial for in vivo application according to the study.

3.8. In vitro transfection

The transfection efficiency of CTS/pDNA and compound **4**/pDNA complexes at different N/P ratios ranging from 1 to 10 was performed on HeLa cell line. pDNA and PEI (25 kDa)/pDNA complex at N/P ratio 10 were used as negative and positive control, respectively. Complex formed with bPEI at N/P ratio 10 was used as a control because N/P 10 was determined to be optimal N/P ratio for transfection without causing massive cell death and with N/P ratios ranging from 9 to 13.5 could produce maximal in vitro transfection efficiency (Lu, Xu, Zhang, Cheng, & Zhuo, 2008). The transfection efficiency of the complexes was first visualized by observation of EGFP (enhanced green fluorescence protein) positive cells using a fluorescence microscope. As shown in Fig. 7A, cells transfected with compound **4c**/pEGFP DNA showed the strongest fluorescent density (f, g, h) while the weakest fluorescent density was displayed on the cells transfected with CTS/pEGFP DNA complexes (b, c, d). Compound **4c**/pDNA complex at N/P ratio 7.0 (Fig. 7A, h) showed highest fluorescent density than that of CTS/pDNA (Fig. 7A, d), compound **4b** and **4c**/pDNA complexes (Fig. 7A, i and j) and even PEI/pDNA complex at N/P ratio 10 (Fig. 7A, e).

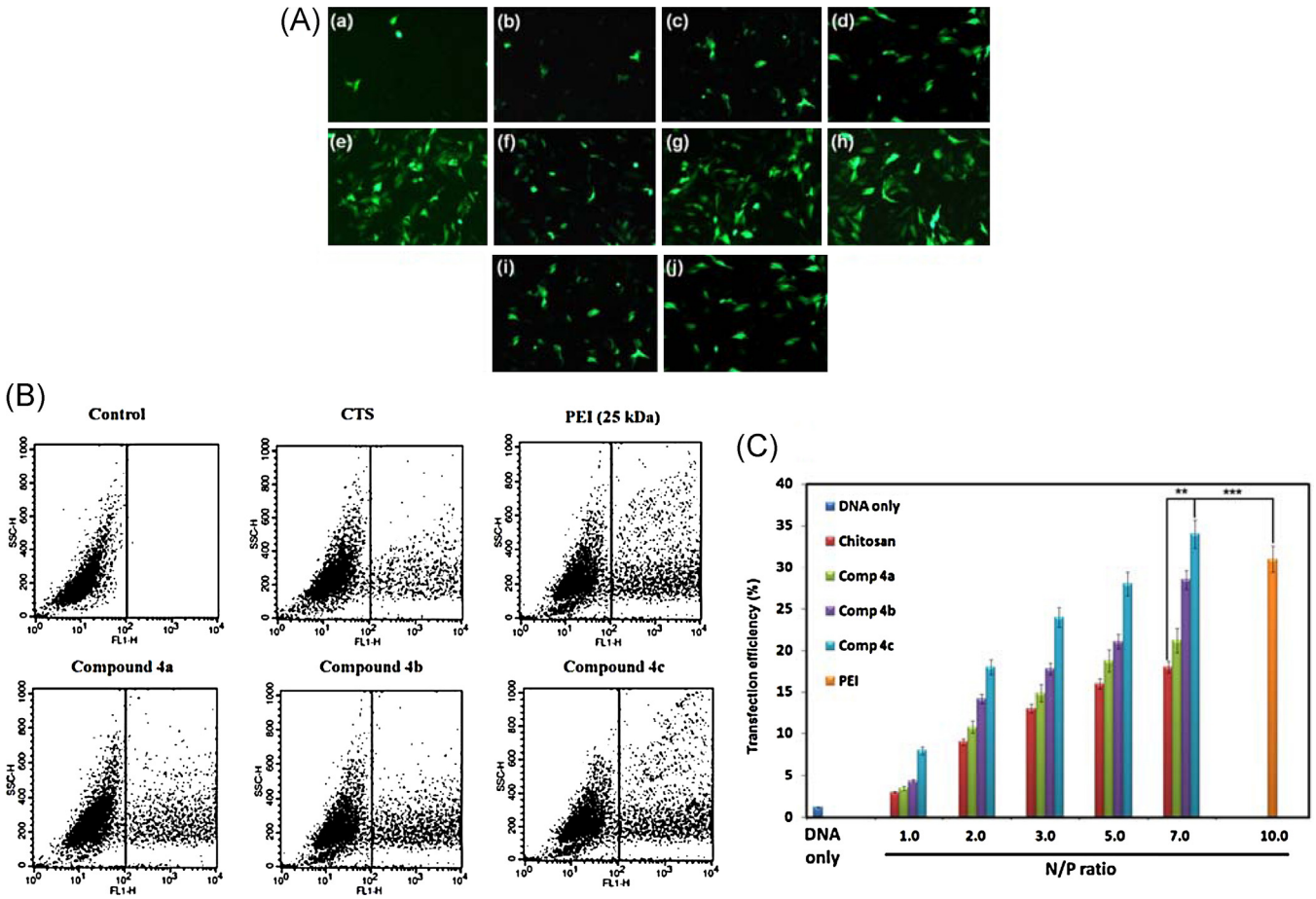

Fig. 7. (A) Typical fluorescence images of HeLa cells transfected by pDNA (a), chitosan/pDNA complexes at N/P ratios 3.0, 5.0 and 7.0 (b, c, d), PEI/pDNA complex at N/P ratio 10 (e), compound **4c**/pDNA complexes at N/P ratios 3.0, 5.0 and 7.0 (f, g, h), and compound **4a**/pDNA (i) and compound **4b**/pDNA (j) complexes at N/P ratio 7.0; (B) representative flow cytometric analysis of GFP-expressing cells after 48 h post transfection by CTS/pDNA complex and compound **4a**, **4b** and **4c**/pDNA complexes at N/P ratios 7.0 and PEI/pDNA complex at N/P ratio 10 and (C) transfection efficiency of pDNA only, CTS/pDNA complexes and compound **4a**, **4b** and **4c**/pDNA complexes at N/P ratios 1.0, 2.0, 3.0, 5.0 and 7.0, and PEI (25 kDa)/pDNA complex at N/P ratio 10 in HeLa cell lines. Data are shown as mean ± SD ($n = 3$). $^{**}p < 0.05$ and $^{***}p < 0.001$.

The transfection efficiencies of the chitosan, compound **4** and PEI on HeLa cells were further quantified by flow cytometry analysis (Fig. 7B). As shown in Fig. 7C, it is found that the transfection efficiency of compound **4**/pDNA complex was increased with increase in the N/P ratios. Compound **4c**/pDNA complex at N/P ratio 7.0 showed highest gene transfection efficiency but the transfection efficiency was decreased for both CTS and chitosan conjugates when the N/P ratios were beyond 7.0 (data not shown). Although, the compounds **4a** and **4b** showed slightly lower transfection efficiency compared to compound **4c** due to lower substitution degree of PAMAM molecules with chitosan. The transfection efficiency of chitosan was significantly increased after conjugating of PAMAM dendrimer with chitosan backbone and the transfection efficiency was reached up to 35% at N/P ratio 7.0, which was higher than PEI with about 31% at N/P ratio 10 whereas, unmodified chitosan showed only 18% transfection efficiency at N/P ratio of 7.0. Recently, N-imidazolyl-O-carboxymethyl chitosan (Shi et al., 2012) was prepared to improve the transfection efficiency of chitosan and 32% transfection efficiency was obtained after imidazolyl conjugation with chitosan. In another study (Lu, Wang, et al., 2009), the transfection efficiency of chitosan was increased after attachment of poyethyleneimine with chitosan. The increased high transfection efficiency is attributed to their ability to destabilize the endosome due to high buffering capacity or proton sponge effect (Benjaminsen, Mattebjerg, Henriksen, Moghimi, & Andresen, 2013) because of the primary, secondary and tertiary amine groups. Similarly, CTS-PAMAM conjugate contains primary, secondary and tertiary amine groups leading to an increase in the buffering capacity of the conjugate and consequently improved the transfection efficiency. Therefore, the synthesized chitosan-PAMAM (G2) conjugate can be used as an effective gene carrier due to its high transfection efficiency and low toxicity.

4. Conclusions

Chitosan-PAMAM conjugate was synthesized by simple substitution reaction of PAMAM dendrimer with chitosan through naphthalimide moiety. After conjugating of PAMAM dendrimer onto chitosan backbone, the water solubility of the conjugate was increased and compound **4c** showed better water solubility than compound **4a** and **4b** due to high substitution degree. DNA complexation ability of the conjugates was significantly improved compared to unmodified chitosan and the chitosan conjugate also formed spherical nanoparticle with pDNA. The conjugate also showed efficient DNA protection from nuclease degradation. The transfection efficiency of CTS-PAMAM conjugate/pDNA complexes increased significantly compared to unmodified chitosan and surpassed the transfection efficiency of PEI at a comparatively lower N/P ratio. In addition to this, the conjugate exhibited excellent blood compatibility with low toxicity even at high concentration (300 μg/mL). Therefore, chitosan-PAMAM conjugate can be used safely as alternate nonviral vector in gene therapy.

Acknowledgements

The authors greatly acknowledge the financial support from University Grants Commission (UGC), India under Rajiv Gandhi National Fellowship program. Finally, the authors thank Dr. Gopal Chakroborty at Biotechnology Department, University of Calcutta to kindly provide his cell culture lab to perform transfection study.

References

Benjaminsen, R. V., Mattebjerg, M. A., Henriksen, J. R., Moghimi, S. M., & Andresen, T. L. (2013). The possible "proton sponge" effect of polyethylenimine (PEI) does not include change in lysosomal pH. *Molecular Therapy*, *21*, 149–157.

Cross, D., & Burmester, J. K. (2006). Gene therapy for cancer treatment: Past, present and future. *Clinical Medicine & Research*, *4*, 218–227.

Daya, S., & Berns, K. I. (2008). Gene therapy using adeno-associated virus vectors. *Clinical Microbiology Reviews*, *21*, 583–593.

Denyer, R., & Douglas, M. R. (2012). Gene therapy for Parkinson's disease. *Parkinson's Disease*, *2012*, 1–13.

Dishart, K. L., Work, L. M., Denby, L., & Baker, A. H. (2003). Gene therapy for cardiovascular disease. *Journal of Biomedicine and Biotechnology*, *21*, 138–148.

Dufes, C., Uchegbu, I. F., & Schatzlein, A. G. (2005). Dendrimers in gene delivery. *Advanced Drug Delivery Reviews*, *57*, 2177–2202.

He, C. X., Tabata, Y., & Gao, J. Q. (2010). Non-viral gene delivery carrier and its three dimensional transfection system. *International Journal of Pharmaceutics*, *386*, 232–242.

Huang, M., Fong, C. W., Khor, E., & Lim, L. Y. (2005). Transfection efficiency of chitosan vectors: Effect of polymer molecular weight and degree of deacetylation. *Journal of Controlled Release*, *106*, 391–406.

Hunter, A. C., & Moghimi, S. M. (2010). Cationic carriers of genetic material and cell death: A mitochondrial tale. *Biochimica et Biophysica Acta*, *1797*, 1203–1209.

Jia, W., & Zhou, Q. (2005). Viral vectors for cancer gene therapy: Viral dissemination and tumor targeting. *Current Gene Therapy*, *5*, 133–142.

Jiang, X., Dai, H., Leong, K. W., Goh, S. H., Mao, H. Q., & Yang, Y. Y. (2006). Chitosan-*g*-PEG/DNA complexes deliver gene to the rat liver via intrabiliary and intraportal infusions. *Journal of Gene Medicine*, *8*, 477–487.

Jewell, C. M., & Lynn, D. M. (2008). Surface-mediated delivery of DNA: Cationic polymers take charge. *Current Opinion in Colloid & Interface Science*, *13*, 395–402.

Kean, T., Roth, S., & Thanou, M. (2005). Trimethylated chitosans as non-viral gene delivery vectors: Cytotoxicity and transfection efficiency. *Journal of Controlled Release*, *103*, 643–653.

Kundu, P. P., & Sarkar, K. (2011). Natural polymeric vectors in gene therapy. In S. Kalia, & L. Avérous (Eds.), *Biopolymers: Biomedical and Environmental application* (pp. 575–604). New Jersey: John Wiley & Sons Inc.

Lechardeur, D., & Lukacs, G. L. (2002). Intracellular barriers to non-viral gene transfer. *Current Gene Therapy*, *2*, 183–194.

Li, S. D., & Huang, L. (2006). Gene therapy progress and prospects: Non-viral gene therapy by systemic delivery. *Gene Therapy*, *13*, 1313–1319.

Lu, B., Sun, Y. X., Li, Y., Zhang, Q., & Zhuo, X. Z. R. X. (2009). N-succinyl-chitosan grafted with low molecular weight polyethylenimine as a serum-resistant gene vector. *Molecular BioSystems*, *5*, 629–637.

Lu, B., Wang, C. F., Wu, D. Q., Li, C., Zhang, X. Z., & Zhuo, R. X. (2009). Chitosan based oligoamine polymers: Synthesis, characterization, and gene delivery. *Journal of Controlled Release*, *137*, 54–62.

Lu, B., Xu, X. D., Zhang, X. Z., Cheng, S. X., & Zhuo, R. X. (2008). Low molecular weight polyethylenimine grafted *N*-maleated chitosan for gene delivery: Properties and in vitro transfection studies. *Biomacromolecules*, *9*, 2594–2600.

Lungwitz, U., Breunig, M., Blunk, T., & Göpferich, A. (2005). Polyethylenimine-based non-viral gene delivery systems. *European Journal of Pharmaceutics and Biopharmaceutics*, *60*, 247–266.

Merdan, T., Kopecek, J., & Kissel, T. (2002). Prospects for cationic polymers in gene and oligonucleotide therapy against cancer. *Advanced Drug Delivery Reviews*, *54*, 715–758.

Miller, A. D. (1998). Cationic liposomes for gene therapy. *Angewandte Chemie International Edition*, *37*, 1768–1785.

Moghimi, S. M., Symonds, P., Murray, J. C., Hunter, A. C., Debska, G., & Szewczyk, A. (2005). A two-stage poly(ethylenimine)-mediated cytotoxicity: Implications for gene transfer/therapy. *Molecular Therapy*, *11*, 990–995.

Morille, M., Passirani, C., Vonarbourg, A., Clavreul, A., & Benoit, J. P. (2008). Progress in developing cationic vectors for non-viral systemic gene therapy against cancer. *Biomaterials*, *29*, 3477–3496.

Mukherjee, S., Davoren, M., & Byrne, H. (2010). In vitro mammalian cytotoxicological study of PAMAM dendrimers – Towards quantitative structure activity relationships. *Toxicology In Vitro*, *24*, 169–177.

Muzzarelli, R. A. A. (2010a). Chitosans: New vectors for gene therapy. In R. Ito, & Y. Matsuo (Eds.), *Handbook of carbohydrate polymers: Development, properties and applications* (pp. 583–604). Hauppauge, NY, USA: Nova Publ.

Muzzarelli, R. A. A. (2010b). Chitins and chitosans as immunoadjuvants and non-allergenic drug carriers. *Marine Drugs*, *8*, 292–312.

Nilsson, P., Iwata, N., Muramatsu, S., Tjernberg, L. O., Winblad, B., & Saido, T. C. (2010). Gene therapy in Alzheimer's disease potential for disease modification. *Journal of Cellular and Molecular Medicine*, *14*, 741–757.

Niidome, T., & Huang, L. (2002). Gene therapy progress and prospects: Nonviral vectors. *Gene Therapy*, *9*, 1647–1652.

Pedroso de Lima, M. C., Neves, S., Filipe, A., Düzgüneş, N., & Simões, S. (2003). Cationic liposomes for gene delivery: From biophysics to biological applications. *Current Medicinal Chemistry*, *10*, 1221–1231.

Pérez-Martínez, F. C., Guerra, J., Posadas, I., & Ceña, V. (2011). Barriers to non-viral vector-mediated gene delivery in the nervous system. *Pharmaceutical Research*, *28*, 1843–1858.

Romano, G. (2007). Development of safer gene delivery systems to minimize the risk of insertional mutagenesis-related malignancies: A critical issue for the field of gene therapy. *Drug News & Perspectives*, *20*, 227–231.

Sadekar, S., & Ghandehari, H. (2012). Transepithelial transport and toxicity of PAMAM dendrimers: Implications for oral drug delivery. *Advanced Drug Delivery Reviews*, *64*, 571–588.

Samal, S. K., Dash, M., Vlierberghe, S. V., Kaplan, D. L., Chiellini, E., van Blitterswijk, C., et al. (2012). Cationic polymers and their therapeutic potential. *Chemical Society Reviews*, *41*, 7147–7194.

Sarkar, K., & Kundu, P. P. (2012). Preparation of low molecular weight N-maleated chitosan-graft-PAMAM copolymer for enhanced DNA complexation. *International Journal of Biological Macromolecules*, *51*, 859–867.

Sarkar, K., Debnath, M., & Kundu, P. P. (2012). Recyclable crosslinked O-carboxymethyl chitosan for removal of cationic dye from aqueous solutions. *Hydrology Current Research*, *3*, 1–9.

Sarkar, K., Debnath, M., & Kundu, P. P. (2013). Preparation of low toxic fluorescent chitosan-graft-polyethyleneimine copolymer for gene carrier. *Carbohydrate Polymers*, *92*, 2048–2057.

Sarkar, K., Srivastava, R., Chatterji, U., & Kundu, P. P. (2011). Evaluation of chitosan and their self-assembled nanoparticles with pDNA for the application in gene therapy. *Journal of Applied Polymer Science*, *121*, 2239–2249.

Shi, B., Shen, Z., Zhang, H., Bi, J., & Dai, S. (2012). Exploring N-imidazolyl-O-carboxymethyl chitosan for high performance gene delivery. *Biomacromolecules*, *13*, 146–153.

Simões, S., Filipe, A., Faneca, H., Mano, M., Penacho, N., Düzgünes, N., et al. (2005). Cationic liposomes for gene delivery. *Expert Opinion on Drug Delivery*, *2*, 237–254.

Stone, D., David, A., Bolognani, F., Lowenstein, P. R., & Castro, M. G. (2000). Viral vectors for gene delivery and gene therapy within the endocrine system. *Journal of Endocrinology*, *164*, 103–118.

Sun, J. Y., Chatterjee, S., & Wong, K. K., Jr. (2002). Immunogenic issues concerning recombinant adeno-associated virus vectors for gene therapy. *Current Gene Therapy*, *2*, 485–500.

Svenson, S., & Tomalia, D. A. (2005). Dendrimers in biomedical applications. *Advanced Drug Delivery Reviews*, *57*, 2106–2129.

Thanou, M., Florea, B. I., Geldof, M., Junginger, H. E., & Borchard, G. (2002). Quaternized chitosan oligomers as novel gene delivery vectors in epithelial cell lines. *Biomaterials*, *23*, 153–159.

Thomas, C. E., Ehrhardt, A., & Kay, M. A. (2003). Progress and problems with the use of viral vectors for gene therapy. *Nature Reviews Genetics*, *4*, 346–358.

Tomalia, D. A., & Frechet, J. M. (2005). Introduction to dendrimers and dendritic polymers. *Progress in Polymer Science*, *30*, 217–219.

Waehler, R., Russell, S. J., & Curiel, D. T. (2007). Engineering targeted viral vectors for gene therapy. *Nature Reviews Genetics*, *8*, 573–587.

Walther, W., & Stein, U. (2000). Viral vectors for gene transfer. *Drugs*, *60*, 249–271.

Wightman, L., Kircheis, R., Rössler, V., Carotta, S., Ruzicka, R., Kursa, M., et al. (2001). Different behavior of branched and linear polyethylenimine for gene delivery *in vitro* and *in vivo*. *Journal of Gene Medicine*, *3*, 362–372.

Zhou, H., Liu, D., & Liang, C. (2004). Challenges and strategies: The immune responses in gene therapy. *Medicinal Research Reviews*, *24*, 748–761.